공학석사학위논문

Stretchable Light-emitting Diodes Using Quantum Dot Color Filters

양자점 색 필터를 이용한 신장성 발광 다이오드

2021년 2월

서울대학교 대학원

에너지환경화학융합기술전공

김상연

양자점 색 필터를 이용한
신장성 발광 다이오드

Stretchable Light-emitting Diodes
Using Quantum Dot Color Filters

지도교수 김 대 형
이 논문을 공학석사 학위논문으로 제출함

2021년 2월

서울대학교 대학원
에너지환경화학융합기술전공
김 상 연

김상연의 석사 학위논문을 인준함
2021년 2월

위 원 장 성 영 은 (인)
부 위 원 장 김 대 형 (인)
위 원 현 택 환 (인)

Stretchable Light-emitting Diodes Using Quantum Dot Color Filters

A THESIS SUBMITTED IN PARTIAL FULFILLMENT OF THE REQUESTMENTS FOR THE DEGREE OF MASTER IN ENGINEERING AT THE GRADUATE SCHOOL OF SEOUL NATIONAL UNIVERSITY

February 2021

By

Sangyeon Kim

Supervisor

Dae-Hyeong Kim

Abstract

Stretchable Light-emitting Diodes Using Quantum Dot Color Filters

Sangyeon Kim

School of Chemical and Biological Engineering

The Graduate School of Chemical Convergence

For Energy &Environment

Seoul National University

The flexible and stretchable display is a key technology in developing a next-generation smart display such as skin-attachable wearable electronics. However, the uniform light-conversion efficiency and light intensity of the display during its stretching are still challenging. Here, we present a stretchable and uniform full-

color quantum dot display for wearable electronics. The quantum dot color based on a low modulus elastomer efficiently converts blue light into red and green light while being stretched. Light diffusion layer containing titania and zinc oxide nanoparticles spread the photons generated by a light-emitting diode to uniformly illuminate a unit pixel of the display. The light conversion and diffusion features were demonstrated by optical characterizations. The results present the potential of the stretchable and full-color quantum-dot display for a next-generation wearable electronics

Keywords: Stretchable electronics, quantum dot, light-emitting diode, full-color display, wearable electronics

Student Number: 2018-23552

Contents

List of Schemes

List of Figures

1. Introduction

As market demand for a wearable smart display for real-time communication of information related to healthcare, social service, and the internet of things has been increased, great attention to deformable displays such as flexible, foldable, and stretchable displays have been made. Although the technology for flexible and foldable displays has been significantly advanced, a few significant limitations still remain. For example, flexible display cannot endure large and repeated deformations such as joint movement. Therefore, the development of a stretchable display that can endure a large strain that is induced by body movement is required for a high-performance and mechanically stable wearable display. A stretchable display can be attached to the skin to deliver various information without an uncomfortable fit.

A variety of technologies such as organic light-emitting diode (LED), polymer LED, and inorganic micro-LED have been studied for developing a stretchable display.[1–9] An intrinsically stretchable display adopting organic and polymer LED as a light-emitting unit has been studied for developing a stretchable display. However, current technology on intrinsically stretchable displays based on organic and polymer LED has a significant limitation. A key material that is essential for the stretchable light-emitting unit hinders carrier transfer, which induces high turn-on voltage and poor light intensity of the stretchable display.

Besides, the technology for intrinsically stretchable display based on organic and polymer LED is still stays in a single-pixel device.

A stretchable inorganic micro-LED display has rigid light-emitting units that have stretchable interconnects. Because the additive material for stretchability is not required, the light-emitting unit performs high turn-on voltage and luminous intensity which could not be enabled in organic and polymer LED-based stretchable displays. Consequently, inorganic micro-LED has an advantage for developing high-performance stretchable displays for wearable electronics. However, light conversion efficiency and intensity at the edge of a unit pixel are significantly lower than those at the center. The size of the unit pixel is considerably larger than the back light-emitting unit owing to spatial gaps emerging from stretchable interconnects. Especially, such degradation of luminous performance is exacerbated as the display is stretched. Therefore, the stretchable display of which performance is high enough compared to conventional display is required in developing a wearable smart display.

Herein, we present a highly stretchable micro-LED display that improves the existing technical difficulties. The light-emitting backplane consists of a micro-LED array. The micro-LEDs integrated with a quantum dot (QD) and Styrene-ethylene-butadiene-styrene (SEBS) nanocomposite color filter build up red-green-blue multicolor pixels. Light diffusion layer composed of titania and zinc oxide nanoparticles, which are bound by SEBS. Optical characterization was executed on The QD-SEBS color filter and light diffusion layer in order to show

the possibility of being used as display material. Also, an optical simulation was carried out to make sure the light from the emitting center is spread evenly across the unit pixel. The implementation of our stretchable multicolor display is expected to open up the future smart display market.

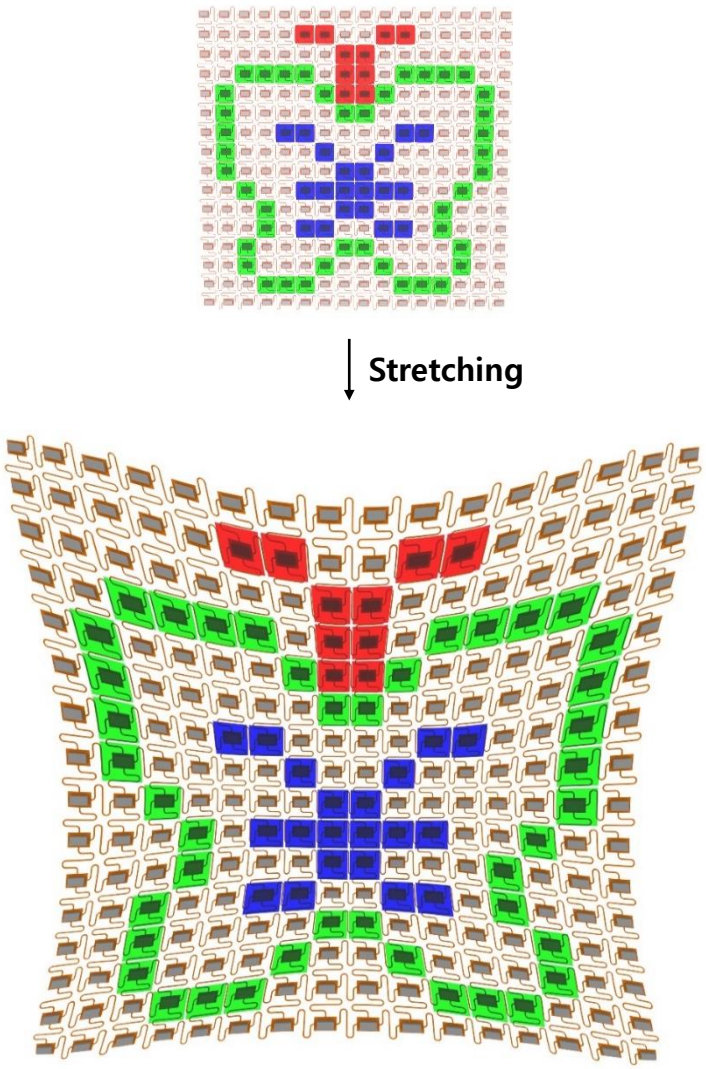

Scheme 1. Schematic illustration of stretchable LED display

2. QD-SEBS nanocomposites as a color filter

2.1 Preparation and integration of QD-SEBS nanocomposites

To produce a QD-SEBS solution, green QD or red QD was dissolved in toluene, and SEBS H1221 was added to the QD solution. The prepared solution was sprayed on the LED with an airbrush. The spray process was carried out on the hot plate of which temperature is over the boiling point of toluene. The schematic image of the integration of QD with micro-LED is illustrated in **Scheme 2**. The image of the micro-LED integrated with color filters made in the above way is presented in **Figure 1.**

To obtain a desired color conversion ratio and maintain the color representation level, a film with uniform thickness and roughness should be formed. The temperature of the hot plate where the spray process is conducted is an important variable over the quality of the film. Therefore, the temperature of the plate was advertently set up after testing under several different temperatures. The SEM images of the films which are made in the various environment are presented in **Figure 2**.

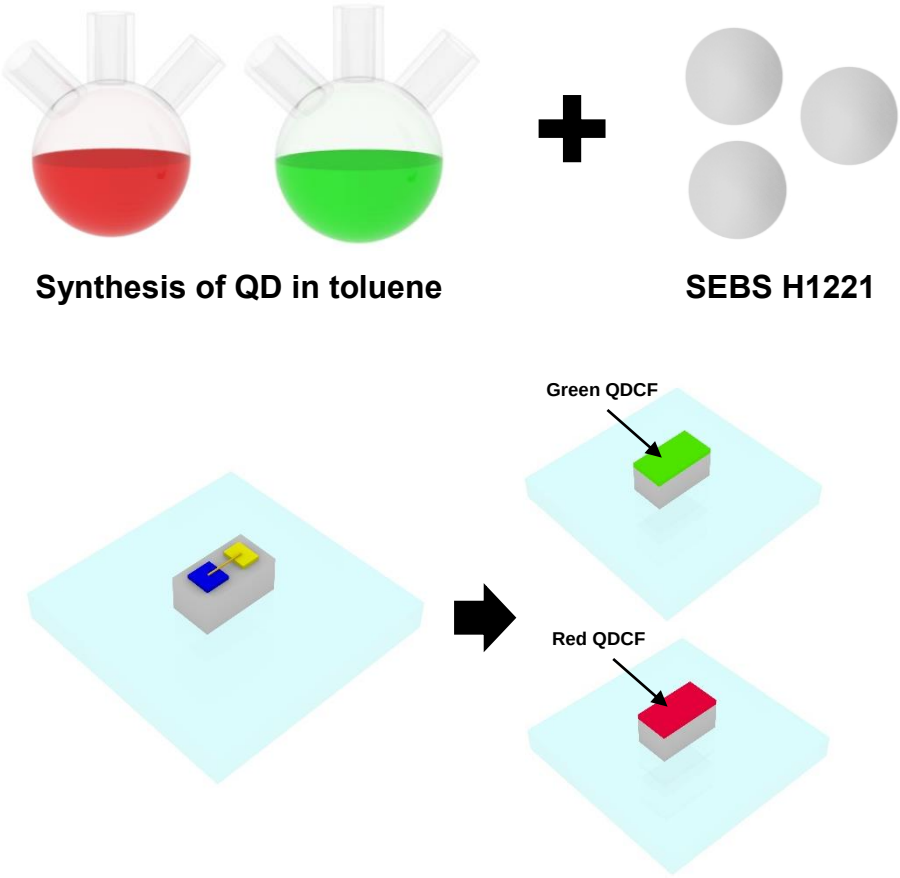

Scheme 2. Schematic illustration of micro-LEDs integrated with color filters

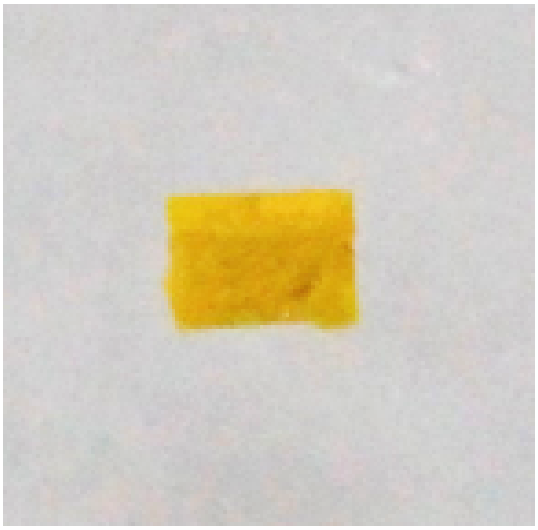

Figure 1. Micro-LED integrated with a green color filter

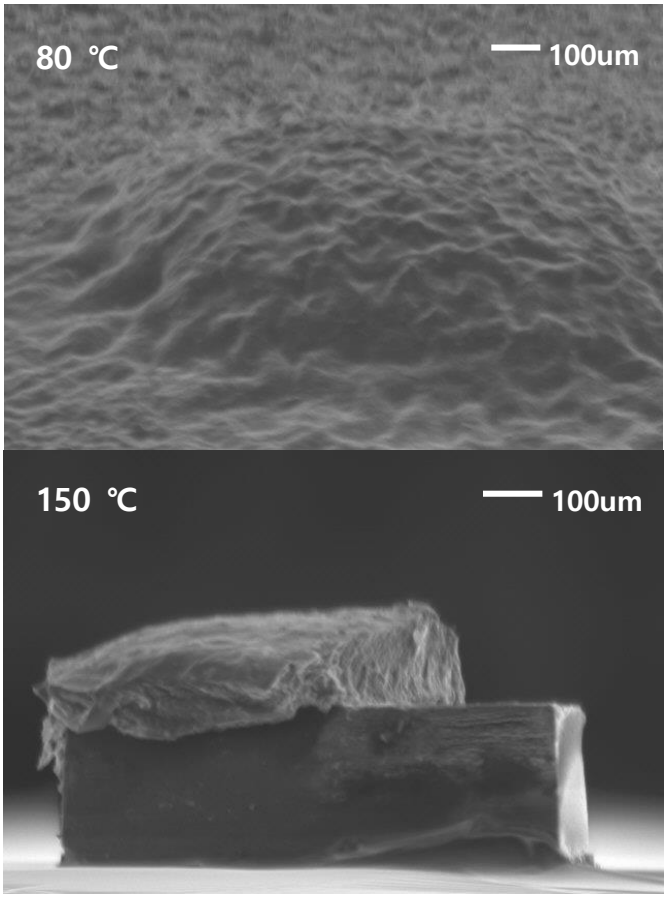

Figure 2. color filters made under different temperatures. The layer is more uniform under the temperature over the boiling point of the solvent

2.2 Optical characterization of a color filter

As we use blue LED for incident light, the color representation would be downgraded if blue light is mixed in green or red pixels. Thus, a sufficiently high color conversion ratio plays a crucial role in display demonstration. To validate the color conversion ability of the color filter, the emission spectrum of the micro-LED which is integrated with the color filter was measured. The obtained spectrum data is presented in **Figure 3** and **Figure 4** for green and red respectively. As shown in Figure, the thicker was the color filter, the higher was the color conversion ratio. However, as it is also important to maintain a certain level of transmittance, the color filter cannot be thickened indefinitely. From the obtained spectrum data, we concluded that a 10um thick color filter shows the most desirable color conversion for both colors.

There is a possibility that the color conversion ratio will be affected as the light intensity changes. Therefore, the emission spectrum of the micro-LED which is integrated with a 10um-thick color filter according to current changes was also measured, and the data results on this are shown in **Figure 5** and **Figure 6** for green and red respectively. According to the spectrum, it is confirmed that the emission spectrum is unlikely to be changed by current changes. Putting the results together, it is considered that the fabricated color filter is enough to be used as a display component.

the emission of red, green, and blue light is successfully presented as shown in **Figure 7.** By using quantum dots as a light-emitting material, excellent and vivid color reproduction could be obtained. The chromaticity diagram over the colors made through our color filters is illustrated in **Figure 8.** Although a slight tilt toward the blue area in red and green vertices, a tricolor triangle which is satisfactory for the display purpose was obtained, as specified in the chromaticity diagram.

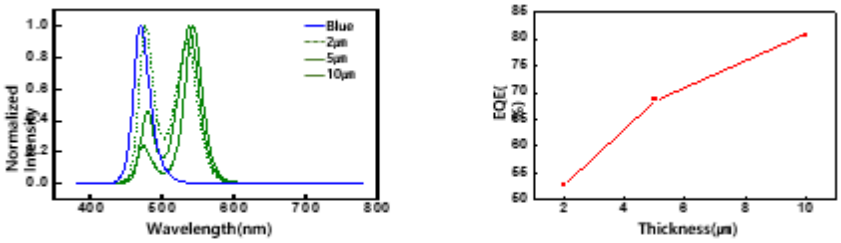

Figure 3. The emission spectra of the micro-LED integrated with a green color filter according to thickness change

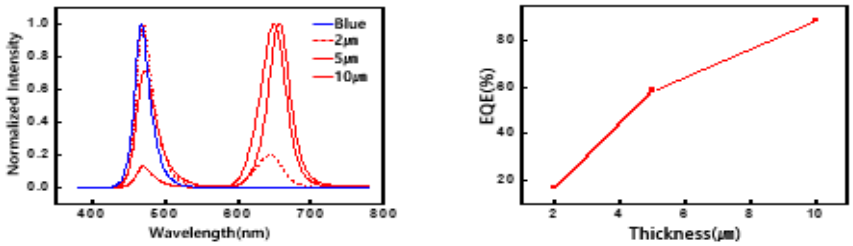

Figure 4. The emission spectra of the micro-LED integrated with a red color filter according to thickness change

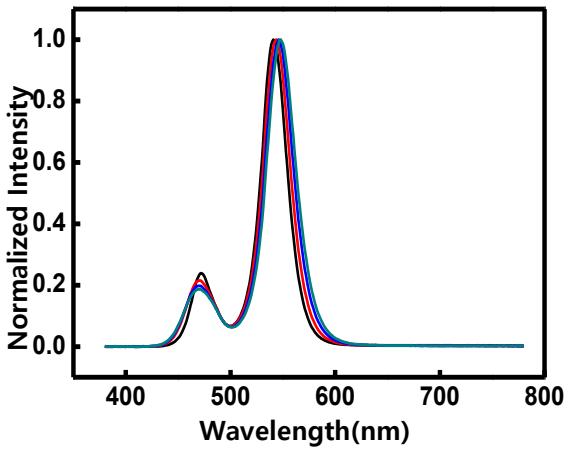

Figure 5. Emission spectrum changes of the micro-LED integrated with a green color filter according to current changes

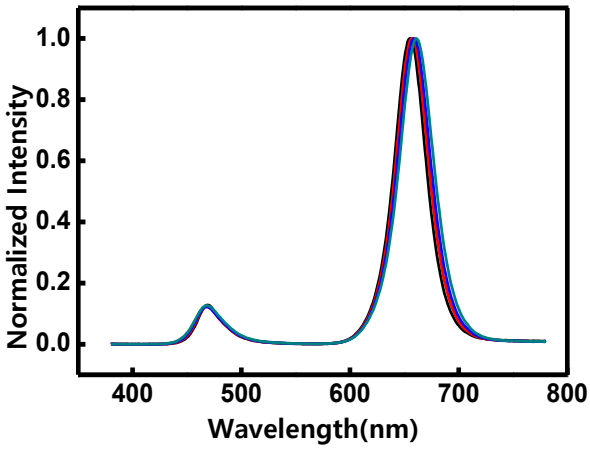

Figure 6. Emission spectrum changes of the micro-LED integrated with a red color filter according to current changes

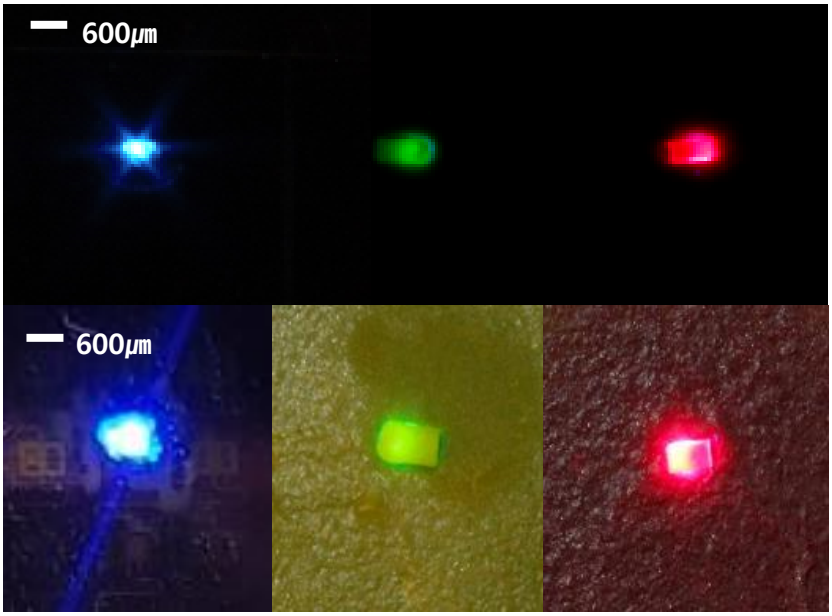

Figure 7. RGB color representation via color filters

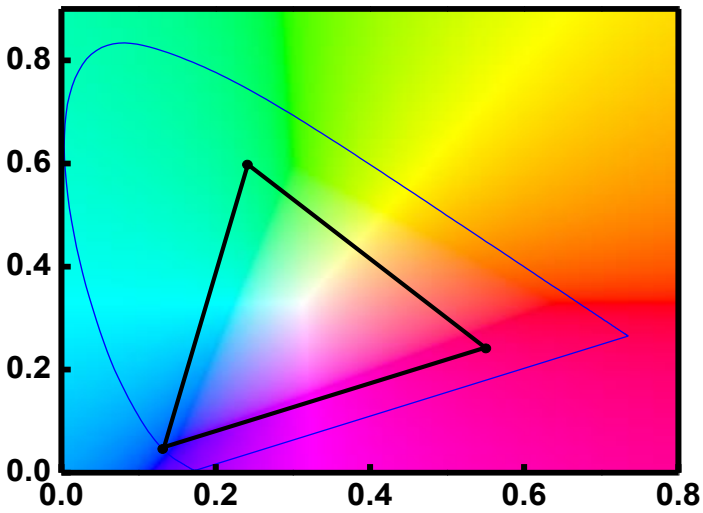

Figure 8. Chromaticity diagram of QD-SEBS color filters

3. SEBS with titania and Zinc oxide nanocomposites as a light diffusion layer

As the neighboring electrode pads for micro-LED are linked by serpentine structure, there was a space between pixels and pixels. Thus, the size of a single-pixel became quite large compared to the size of an emitting center. To fill the space with light in a complete manner, the integration of the light diffusion layer is essential. Moreover, the performance of the light diffusion layer is exceptionally significant for successful display implementation. The schematic diagram of the light diffusion layer is illustrated in **Scheme 3**. In this chapter, the fabrication and properties of the light diffusion layer are to be described.

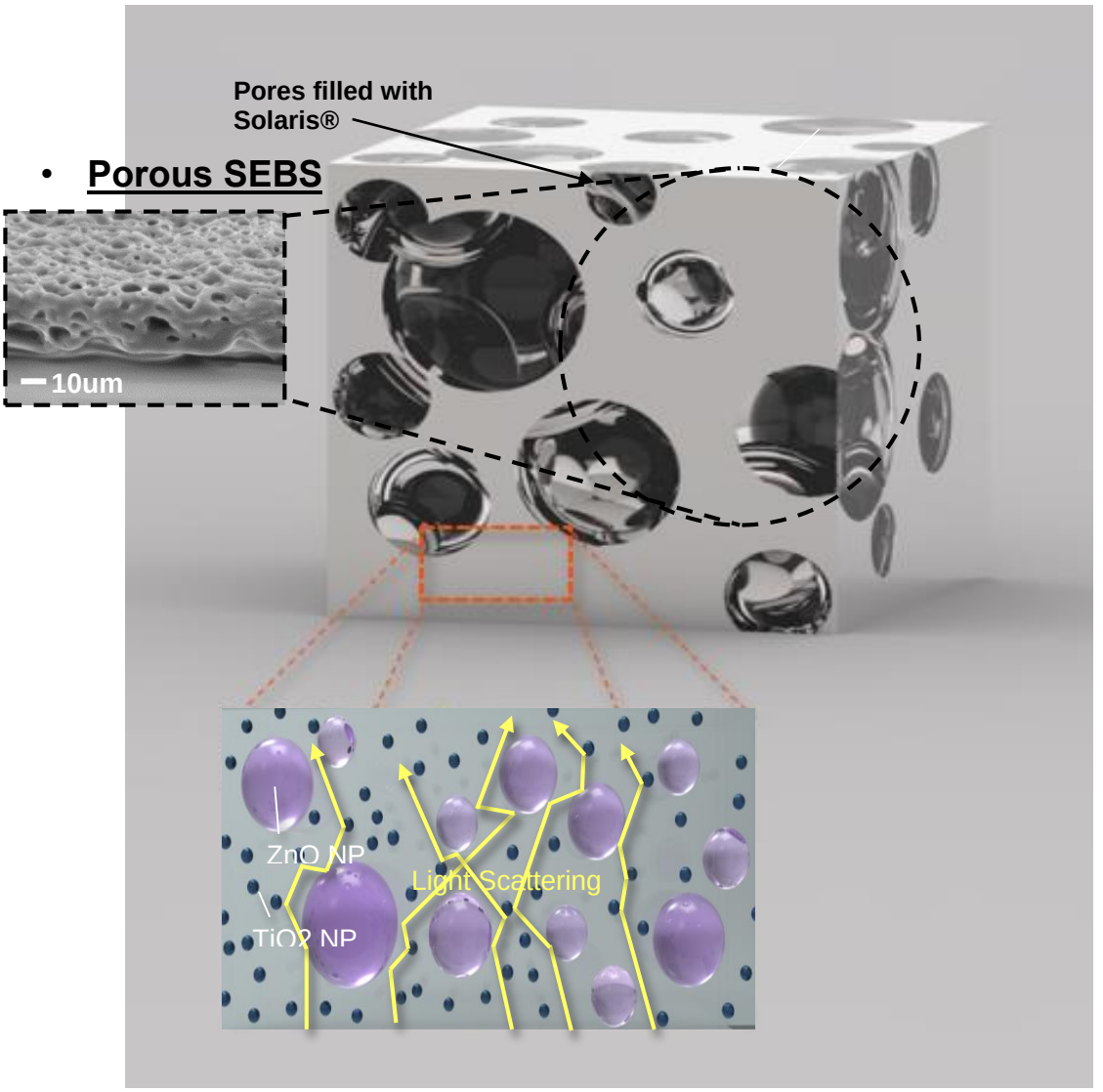

Scheme 3. Schematic diagram of the light diffusion layer

3.1 Fabrication of the light diffusion layer

When SEBS is dissolved in the mixture of two different solvents which are hardly miscible with each other, a porous SEBS structure is made by drying away all solvents. The size of the pores depends on the type of solvents, and the most conspicuous pores are formed by adopting chloroform and isopropyl alcohol as solvents. The resulting porous SEBS shows brilliant white color. As porous SEBS has its scattering centers in itself as well as the capacity to bind scattering nanoparticles, it is good for use as a substrate material of the light diffusion layer. SEM image and optical image are presented in **Figure 9.**

To produce the solution for the light diffusion layer, self-made titania and zinc oxide nanoparticles were dissolved in porous SEBS solution. Similar to the case of a color filter, the prepared solution was sprayed on the substrate. The SEM image of the spray-coated light diffusion layer is presented in **Figure 10.**

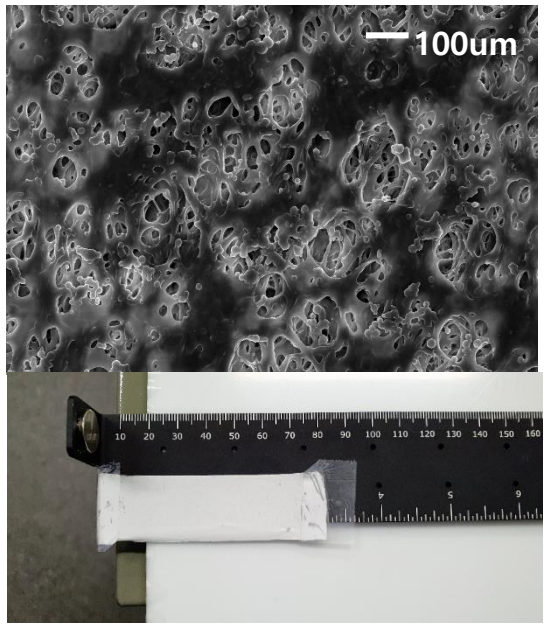

Figure 9. SEM image and optical image of porous SEBS

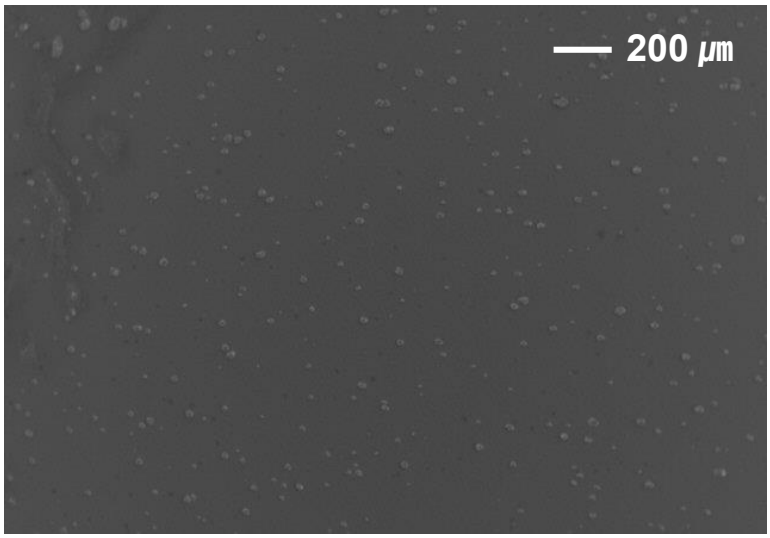

Figure 10. SEM image of the surface of a light diffusion layer

3.2 Characterization of the light diffusion layer

To validate the light scattering ability of the light diffusion layer, haze and transmittance were measured for bare porous SEBS and light diffusion layer respectively, and the resulting data is presented in **Figure 11** and **Figure 12.** As shown in the data, the haze value of a light diffusion layer is remarkably higher than that of porous SEBS. On the other hand, the transmittance value of the light diffusion layer is comparably lower than that of porous SEBS. From the result, we can find that there is an offset between haze and transmittance. Thus, the concentration of light scattering particles is needed to be optimized to maintain enough haze and transmittance at the same time.

The Light scattering effect of the light diffusion layer was also confirmed as an optical image, and it is presented in **Figure 13.** It is shown that the area of the light passing through the light diffusion layer is much wider than the light from a bare LED. From these data, we can conclude that the light diffusion layer is optically well-organized.

Finally, a mechanical characterization for the light diffusion layer was carried out. Unlike color filters, the light diffusion layer should be stretched by itself. Thus, the maximum elongation value is important for the light diffusion layer. To achieve this, the stress-strain curve for a light diffusion layer was measured, and the maximum elongation data was over 100% stretching.

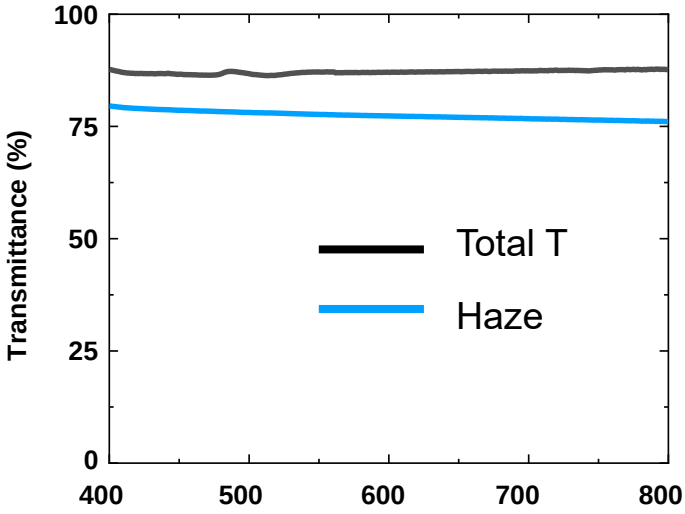

Figure 11. Transmittance and haze of bare porous SEBS

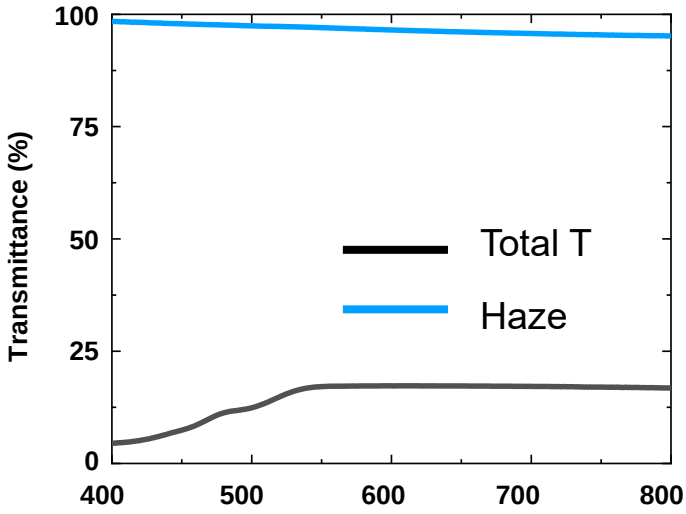

Figure 12. Transmittance and haze of porous SEBS with NPs

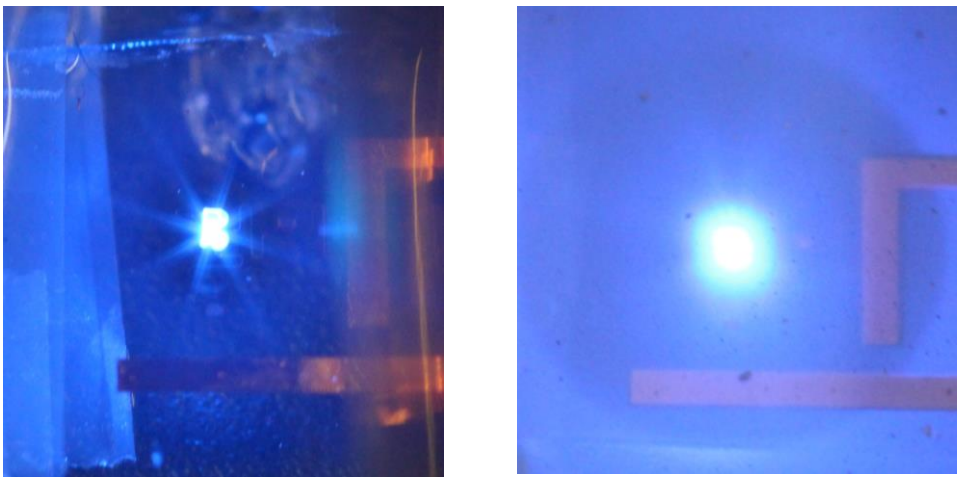

<w/o diffusion layer> <w/ diffusion layer>

Figure 13. Light scattering effect of a light diffusion layer

3.3 Optical simulation of the light diffusion layer

In addition to optical characterization, optical simulation for a light diffusion layer was performed to prove its light scattering ability theoretically. The light diffusion ability of the light diffusion layer was further demonstrated by the optical simulation executed in **Figure 14**. The upper image presents the simulation result done without a light diffusion layer, and the lower image of the simulation result was obtained with the light diffusion layer. Unlike the upper image, the lower image shows that the light passing through the light diffusion layer has a uniform level of intensity throughout the face. This simulation result validates the performance of the light diffusion layer. An additional simulation displayed in **Figure 15** shows the variation of light intensity according to scattering particle density, and the information would be used for optimizing the concentration of scattering particles in the nanocomposites. The concentration should be advertently regulated because there is an offset between light diffusion and transmittance.

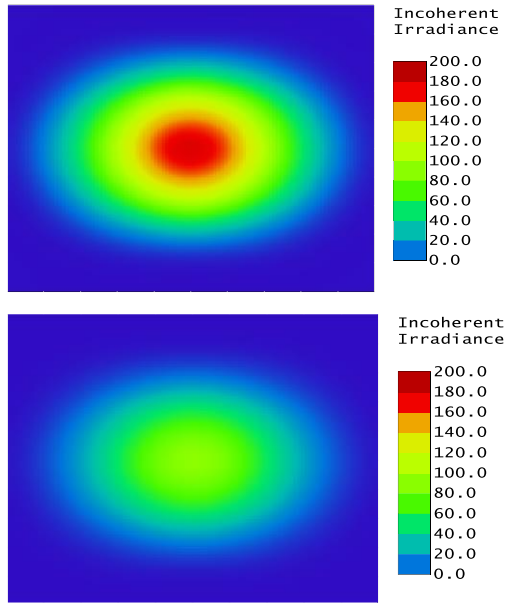

Figure 14. Light diffusion effect visualized by optical simulation

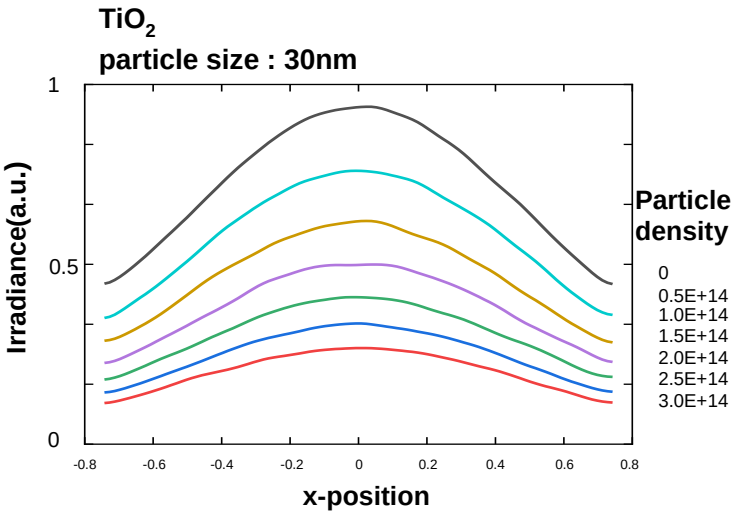

Figure 15. Light diffusion effect according to scattering particle density

4. Electrode backplane with a serpentine structure

4.1 Fabrication of the electrode backplane

To fabricate a stretchable electrode backplane, First, a photolithographic process was performed on a silicon oxide wafer. The detailed fabrication process was described in the experimental section. After that, the electrode was transferred on Solaris substrate which is a highly stretchable and transparent elastomer. Then, the electrode backplane is stretchable by itself.

A stretchable LED array was achieved by put micro-LEDs integrated with a color filter on the stretchable electrode backplane. To obtain the LED array as an aligned form, a metal mask with holes that have the same size as a micro-LED was aligned in advance, and subsequently, LEDs were inserted into the mask holes. Finally, a connection of the LEDs with the electrode was made by using silver epoxy as soldering material. The total process flow is illustrated in **Scheme 4.**

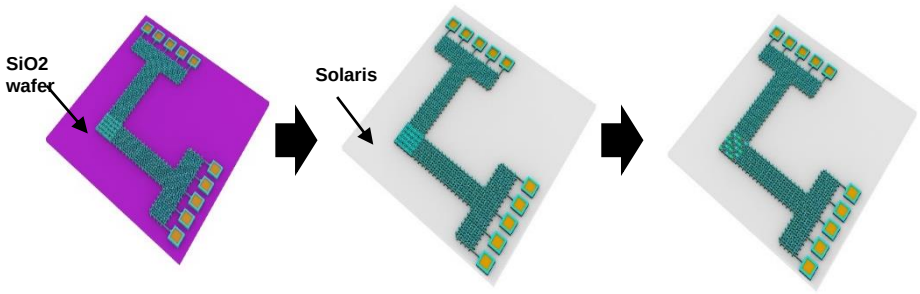

Scheme 4. Schematic images of a fabrication process of a stretchable backplane

4.2 Mechanical characterization of the stretchable backplane

A**s** the serpentine structure of the backplane electrode is the most crucial factor which determines the maximum stretchability of the entire device, a stretchability test should be performed for the stretchable backplane, in order to check whether cracks or breaks occur in the lines. As 60% stretchability is considered enough elongation for the stretchable display, mechanical characterization of stretchable backplane was executed by stretching to 60% in a 1-d stretcher. The image of the stretching test is presented in **Figure 16**, and as shown, there was no observed mechanical failure in the line and the substrate. Overall, It can be concluded that our stretchable backplane has enough stretchability to be used for stretchable display.

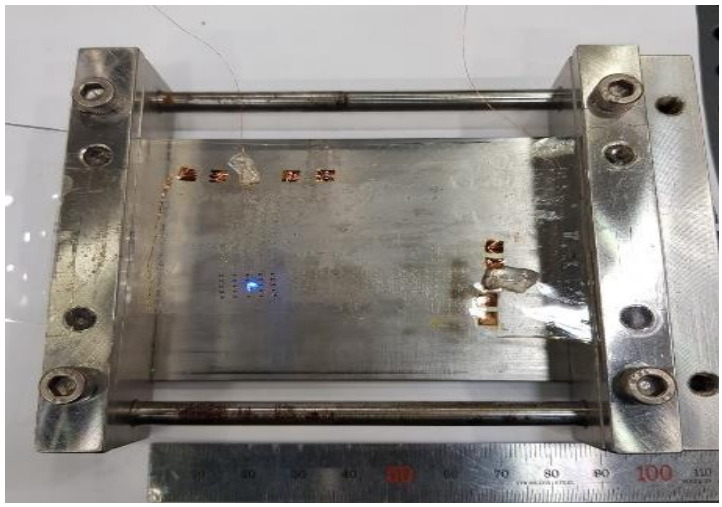

Figure 16. Optical image of stretching test of the stretchable backplane

5. Experimental Section

5.1 Color filters

Single color QD was dissolved in toluene by 0.36g/ml concentration, and add SEBS into QD solution by 0.10g/ml toluene. Stir the solution at 300 rpm for 1 hour for QD and SEBS to be completely dissolved by toluene. After the solution was made, QD-SEBS solution was spray-coated onto the substrate with Iwata HP-CH airbrush on a 135℃ hot plate.

5.2 A diffusion layer

Porous SEBS solution was made by putting SEBS into chloroform by 0.10g/ml and adding isopropyl alcohol by volume ratio of (V_{CCl4}: V_{IPA} = 5: 2). Sonicate the solution at 40℃ for 1 hour. Titania and zinc oxide nanoparticles were synthesized in a toluene medium. By the addition of nanoparticles into porous SEBS solution, light diffusion layer solution was put together. After that, the diffusion layer solution was spray-coated onto the substrate with Iwata HP-CH airbrush on a 135℃ hot plate.

5.3 An electrode Backplane

Poly(pyromellitic dianhydride-co-4,4′-oxydianiline), amic acid solution (Sigma Aldrich) polyimide(PI) was spin-casted on a silicon oxide wafer at 3000rpm for 30seconds. PI was immediately annealed at 150℃ for 15 minutes

and at 250℃ for 1 hour. The 1st PI layer surface was treated by Reactive Ion Etching(RIE) for 1 minute with 50W, 0.1torr in 100sccm oxygen flow. After that, 2um Copper(Cu) layer was laminated on the 1st PI layer by thermal evaporation. The 1st Cu layer was patterned by photolithography using AZ5214 photoresist. After patterning of the 1st Cu layer, a 2nd PI layer was spin-coated at the same condition as the 1st PI layer. The 2nd PI layer was annealed in a glove box to prevent Cu oxidation. After annealing, the 2nd PI layer was also treated by RIE at the same condition as the 1st PI layer. After that, the 2nd Cu layer was deposited on the 2nd PI layer by thermal evaporation. The 2nd Cu layer was patterned in the perpendicular direction with the 1st Cu layer by the photolithographic process using AZ5214 photoresist. After patterning of the 2nd Cu layer, a 3rd PI layer was spin-coated at the same condition as the 1st PI layer. The 3rd PI layer was annealed in a glove box. After annealing, the 3rd PI layer was also treated by RIE at the same condition as the 1st PI layer. After that, an aluminum(Al) layer was deposited onto the 3rd PI layer. Al layer was patterned by the photolithographic process using AZ5214 photoresist. The aluminum layer acts as a metal mask. After patterning the Al layer, three PI layers were etched by RIE for 15 minutes with 150W, 0.1torr in 100sccm oxygen flow. After etching PI, the aluminum metal mask was etched by an aluminum etchant.

6. References

1. Larson, C. *et al.* Highly stretchable electroluminescent skin for optical signaling and tactile sensing. *Science (80-.).* **351**, 1071–1074 (2016).

2. Shin, H. *et al.* Stretchable Electroluminescent Display Enabled by Graphene-Based Hybrid Electrode. *ACS Appl. Mater. Interfaces* **11**, 14222–14228 (2019).

3. Wang, Y. *et al.* A highly stretchable, transparent, and conductive polymer. *Sci. Adv.* **3**, 1–11 (2017).

4. White, M. S. *et al.* Ultrathin, highly flexible and stretchable PLEDs. *Nat. Photonics* **7**, 811–816 (2013).

5. Sekitani, T. *et al.* Stretchable active-matrix organic light-emitting diode display using printable elastic conductors. *Nat. Mater.* **8**, 494–499 (2009).

6. Kim, R. H. *et al.* Waterproof AlInGaP optoelectronics on stretchable substrates with applications in biomedicine and robotics. *Nat. Mater.* **9**, 929–937 (2010).

7. Xu, J. *et al.* E (1 , 2),. **64**, 59–64 (2017).

8. Yang, C. H., Chen, B. H., Zhou, J. X., Chen, Y. M. & Suo, Z. G. Electroluminescence of Giant Stretchability. *Adv. Mater.* **28**, 4480–4484 (2016).

9. Hong, J. H. *et al.* The first 9.1-inch stretchable AMOLED display based on LTPS technology. *Dig. Tech. Pap. - SID Int. Symp.* **48**, 47–50 (2017).